Precise geometry of the anterior chamber of the eye by means of OCT imaging

Precise geometry of the anterior chamber of the eye by means of OCT imaging

Marta Skrok,[*1] Damian Siedlecki,[1] and David Alonso-Caneiro[2]

[1]*Department of Optics and Photonics, Wroclaw University of Science and Technology, Wybrzeże Wyspiańskiego 27, 50-370 Wrocław, Poland,*

[2]*School of Optometry and Vision Science, Queensland University of Technology, Victoria Park Road, Kelvin Grove QLD 4059 Brisbane, Australia*

Received May 31, 2018; accepted July 02, 2018; published September 30, 2018

Abstract—Nowadays medicine highly relies on non-invasive optical diagnostic methods. A likewise situation is in the case of ophthalmology, especially in diagnosis of anterior segment eye diseases, where optical coherence tomography (OCT) plays an inestimable role. OCT devices can do fast, painless measurements of the anterior segment of the eye. Nonetheless, it should be remembered that OCT images are burdened with an optical distortion and they do not reflect the true geometry of the eye. This study presents an algorithm for correcting the distortion in OCT images and reflecting the true parameters of the anterior segment of the eye.

Raw OCT data suffer from optical distortion, since the internal anatomical structures of the eye are imaged through the preceding structures [1-2]. Like in many other interferometric techniques, OCT records only the optical path differences and the refraction phenomenon is not taken into account. Therefore, in order to reconstruct the real geometrical parameters of the anterior segment with a reliable precision, optical distortion correction needs to be applied.

The images were captured with the use of SS-OCT Casia 2 (Tomey®, Japan). This commercial device allows detailed imaging of the whole anterior segment of the eye (including both the front surface of the cornea and the back surface of the lens) with an axial resolution of 10μm (in tissue) and a transversal resolution of 30μm. These data were put through numerical analysis procedures developed in Matlab. The first element of the analysis was a detailed and reliable segmentation of the captured images and finding the coordinates of points that create each structure of the anterior segment of the eye (Fig. 1a). The details of the processing method have been presented elsewhere [3-4]. The next step was to find the most optimal algorithm for smoothening the segmented data. For this purpose we have tested several methods of smoothening the data and the best results were observed for the data smoothed with the use of local regression using weighted linear least squares and a 2nd degree polynomial model – loess method – with the span parameter equal to 0.099. The smoothening procedure was applied as follows: raw data were smoothened with the parameters mentioned above; then the difference between the raw data and the smoothened was calculated and smoothening was applied to the result. The final result, which was used for further calculations, was obtained by adding the data from the first smoothening and the smoothened difference.

* E-mail: marta.skrok@pwr.edu.pl

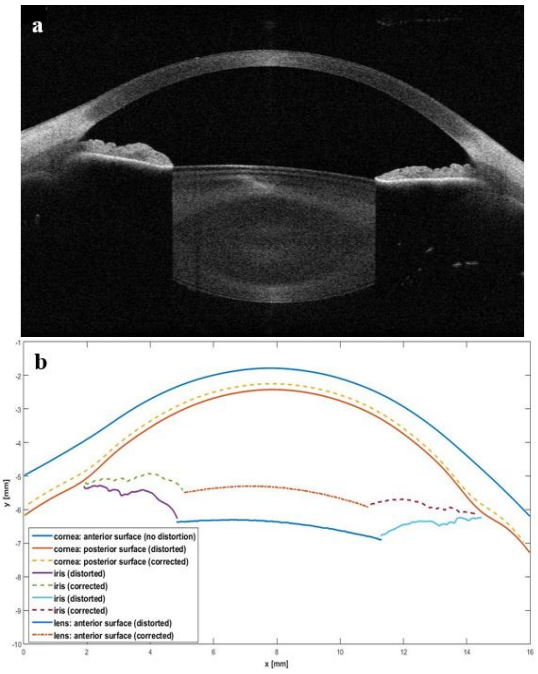

Fig. 1. a) Raw OCT image and b) comparison of the distorted and corrected data.

The next step was getting rid of the optical distortion from the segmented OCT data. The algorithm created for this purpose was strictly based on the law of refraction. First, the axial distance between consecutive eye structures seen on OCT images was calculated. These distances represent the optical path between the consecutive structures of the eye. The geometrical path was obtained by division of the optical path by the index of refraction for $\lambda = 1310$nm, namely: $n = 1.3710$ for cornea and $n = 1.3311$ for aqueous humor (the chromatic

dispersion was taken into account according to Ref. [5]). Then the exact angle of incidence was determined due to the smoothening procedure applied to the refracting surface (anterior and posterior) in the prior stage. Then the refracted ray angle was calculated and a section of the length equal to the geometrical path along the refracted ray was marked. The end of this section indicates the real point on the consecutive surface of the eye. If one applies this procedure to all the rays across the OCT data, one can obtain a set of such points that belong to the surface of the eye structures. This way it is possible to retrieve the true coordinates of points building each surface of the eye structures and reconstruct the true geometry of the anterior segment of the eye (Fig. 1b).

Figure 2 shows the parameters of the anterior segment of the eye which were possible to reconstruct after optical distortion correction.

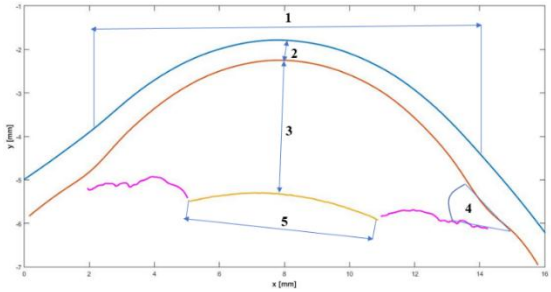

Fig. 1. The geometric parameters of the anterior segment of the eye: 1- diameter of the cornea, 2- depth of the cornea, 3- central depth of the anterior chamber, 4- the magnitude of the irido-corneal angle, 5- diameter of the lens.

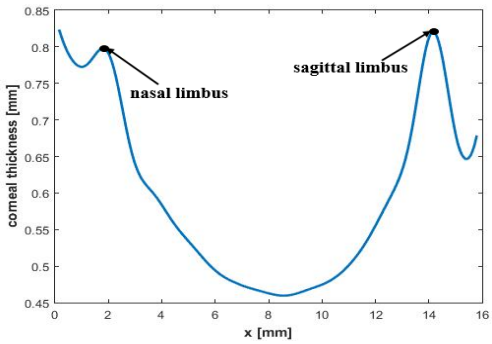

Fig. 2. Plot of the corneal thickness.

The thickness of the cornea was estimated as a geometrical distance between the anterior and posterior surface of the cornea, respectively, along the direction normal to the shape of the anterior surface across the full set of data. An exemplary map of corneal thickness is shown in Fig. 3. This graph enables further estimation of some other characteristics related to the cornea.

One of these characteristics is the corneal limbus – a corneo-scleral junction, in other words, a place in which cornea turns into sclera. On the graph showing the thickness of the cornea, the limbus can be recognized as the points where the curve reaches local maximal values. As expected, the cornea has its smallest thickness in the apex (which is placed in the central part of the plot) and its thickness increases with the distance from the center to both the nasal and sagittal directions. The thickness reaches its maximum in the area of corneal limbus. Figure 4 shows the plot of the curvature of the anterior corneal surface. This plot also gives the estimates of the corneal limbus: these are the points where the corneal curvature changes its sign from positive to negative. The diameter of the cornea can be estimated as the distance between the points of corneal limbus on the nasal and sagittal side.

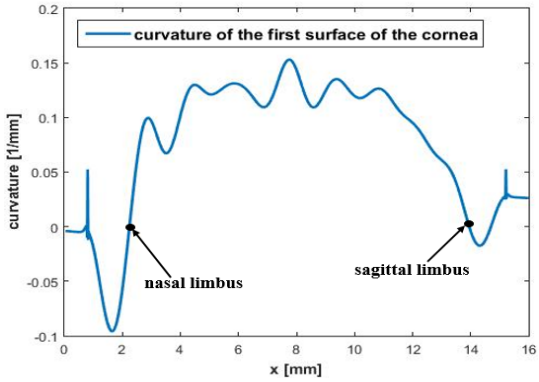

Fig. 3. Map of the curvature of the first surface of the cornea.

Certain regularities can be noticed while comparing Figs. 3 and 4: the maximum value for the curvature corresponds to the point of the minimal thickness where the corneal apex is. Estimated localization of the corneal limbus gives the same outcome with both methods: the first one based on the thickness graph of the cornea, the second one based on the graph of curvature. The width of the pupil was calculated by simple measuring the distance between the opposite points of the lens seen on the OCT images.

The most complicated element of the analysis was to determine the magnitude of the irido-corneal angle. This parameter is of critical importance, because the measure of the irido-corneal angle is the basic test in the diagnostics of glaucoma. The irido-corneal angle lays in a significant distance from the optical axis, thus the raw OCT image in this point is significantly deformed by optical distortion, which results in unreliable values of the irido-corneal angle. The application of the optical distortion correction algorithm mentioned above enabled reliable estimation of the irido-corneal angle.

TIA (Trabecular-Iris Angle) method was used for estimation of the irido-corneal angle, which is based on a direct measure of the angle [6]. In this method the angle is limited by the point placed on the cornea in a 500µm distance from the angle apex and the corresponding point on the iris (crossing with the perpendicular straight heading from the cornea). Figure 5 presents the scheme of this method. The irido-corneal angle was determined for

the images before and after removal of optical distortion and the results were compared. As it turned out, the differences between these measures are significant, which is in agreement with the anticipated results, namely that the distortion in this particular region has a considerable influence on the quantification of the OCT data.

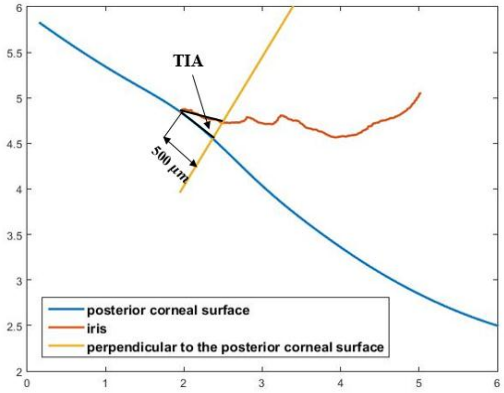

Fig. 4. TIA method of measurement of the irido-corneal angle.

Table 1 shows exemplary values for the width of the cornea, size of the pupil, depth of the anterior segment of the eye at the point of the corneal apex, estimated for 5 different sets of OCT data captured for 5 different subjects. The obtained values are in agreement with the literature data for healthy subjects, for which the diameter of the cornea is 12.25±0.49mm [7], the depth of the anterior segment of the eye is from 2.73±0.20mm to 3.18±0.31 mm [8], and the diameter of the pupil in scotopic conditions is 6.09±1.00 mm [9].

Table 1. Geometry of the anterior segment of the eye: 1- diameter of the cornea, 2 - central depth of the anterior chamber (distorted), 3 - central depth of the anterior chamber (corrected), 4 - diameter of the lens (distorted), 5 - diameter of the lens (corrected).

Number of subject	1 [mm]	2 [mm]	3 [mm]	4 [mm]	5 [mm]
1	12.21	3.24	2.57	6.35	5.80
2	12.74	3.61	2.86	5.55	4.93
3	13.28	3.77	2.98	5.92	5.26
4	12.54	4.11	3.24	5.88	5.21
5	11.41	3.94	3.08	6.47	5.79

The indicated diameter of the pupil is compared with low light conditions, because these are the conditions prevailing while examining with an OCT Casia 2, which uses infrared light.

All of the obtained values, reconstructed from the OCT data corrected from the optical distortion, are within the literature data limits. Table 2 shows the differences between the values of the irido-corneal angle computed from raw data (burdened with distortion) and the data corrected from optical distortion. The results obtained in the current study are in agreement with the value of 42.2±11.3º obtained in other studies and measured for healthy subjects by means of similar methods [10].

It appears that the values of the irido-corneal angles retrieved directly from raw OCT data are heavily overestimated. That fact is crucial because inaccurate estimation of the irido-corneal angle can prevent early detection of angle closure glaucoma (ACG).

Table 2. The magnitude of the iridocorneal angle.

Number of subject	Iridocorneal angle (distorted) [deg]	Iridocorneal angle (corrected) [deg]	Difference [%]
1	31.78	22.17	30
2	29.82	20.73	30
3	51.06	30.18	41
4	43.72	25.70	41
5	39.46	19.51	51

The presented algorithm allows to retrieve a repeatable, precise and reliable parameters of the anterior segment of the eye. Due to the correction of optical distortion in OCT images, it was possible to reconstruct the true geometry of the anterior segment. Basically, the presented study is an introduction to further research of the pulsational dynamics of anterior segment geometry. In order to facilitate the analysis of the dynamical changes that appear in the anterior segment of the eye, it was important that the operation of the algorithm be fully automated, and this goal was achieved. The upcoming step will be an analysis of the whole registered video sequence and an analysis of the dynamics of geometry of the anterior segment of the eye, and relating it with blood pulsation in the eye.

References

[1] A. Podoleanu, I. Charalambous, L. Plesea, A. Dogariu, R. Rosen, Phys. Med. Biol. **49**(7), 1277 (2004).
[2] S. Ortiz, D. Siedlecki, I. Grulkowski, L. Remon, D. Pascual, M. Wojtkowski, S. Marcos, Opt. Expr. **18**, 2782 (2010).
[3] F. LaRocca, S.J. Chiu, R.P. McNabb, A.N. Kuo, J.A. Izatt, S. Farsiu, Biom. Opt. Expr. **2**(6), 1524 (2011).
[4] S.A. Read *et al*., Sci. Rep. **6**, 33796 (2016).
[5] S.R. Uhlhorn, D. Borja, F. Manns, J.-M. Parel, Vision Res. **48**(27), 2732 (2008).
[6] R. Koprowski, Z. Wróbel, S. Wilczyński, A. Nowińska, E. Wylęgała, Biomed. Eng. Online **12**, 40 (2013).
[7] D.P. Pinero, A.B. Plaza Puche, J.L. Alio, J. Cataract Refract. Surg. **34**, 126 (2008).
[8] B. Urban, M. Krętowska, M. Szumiński, A. Bakunowicz-Łazarczyk, Klinika Oczna **114**(1), 18 (2012).
[9] L. Chen, D. Chernyak, Invest. Ophthalmol. Vis. Sci. **54**, 1524 (2013).
[10] D. Monsalvez-Romin, A.J. del Aguila-Carrasco, T. Ferrer-Blasco, J.J. Esteve-Taboada, R Montes-Mico, Int. J. Ophthalmol. **10**(10), 1614 (2017).

